

Astrometric Shifts in the OGLE-1 Microlensing Events

David M. Goldberg and Przemysław R. Woźniak
 Princeton University Observatory, Princeton, NJ 08544-1001
 email: (goldberg, wozniak)@astro.princeton.edu

ABSTRACT

We measure the astrometric shifts of the light centroids for the microlensing events in the OGLE-1 database. Of the 15 consistently detected events, 7 had significant shifts which we were able to measure with a fair degree of confidence. Those events with large shifts are also expected to be unresolved with a background “blend”, and thus, we suggest that we have identified events in the OGLE-1 catalog which are strongly blended. Though we concentrate on the OGLE-1 database, and use the DoPHOT package in order to perform our analysis, we suggest that this shift is a generic effect, and should be observable in any crowded field.

Subject headings: Gravitational Microlensing

1. Introduction

The search for gravitational microlensing events has been very successful. To date, over 100 candidate events have been detected, primarily by the MACHO collaboration (Alcock et al. 1993), but also significantly by the OGLE (Udalski et al. 1992), DUO (Alard 1996a), and EROS (Palanque-Delabrouille et al. 1997) collaborations. In order to maximize event rates, the searches take place toward crowded fields such as the Galactic bulge and the LMC (Alcock et al. 1996).

While searches toward crowded fields allow for a large number of detections, this also makes it highly likely that an observed star will have several contributing unresolved sources. Since only one of these sources is lensed at any given time, events will, in general, be blended (Di Stefano & Esin 1995; Alard 1997; Woźniak & Paczyński 1997; Han 1997; Goldberg 1998).

For any event, we define the blending fraction, f as:

$$f \equiv \frac{F_s}{\sum_i F_i} = \frac{F_s}{F_0} \leq 1, \quad (1)$$

where F_s is the flux from the lensed star, F_i is the flux from each of the contributing stars in the point spread function (PSF), and F_0 is the total flux from the observed object.

If an event is blended, a measurement of the microlensing magnification, $A_{obs}(t)$, will be a systematic underestimate of the true magnification of the source star, $A(t)$:

$$A_{obs}(t) = 1 - f + A(t)f \leq A(t) . \quad (2)$$

For a single lens microlensing event, $A(t)$ evolves in a straightforward way (Paczynski 1986; 1996):

$$A(t) = \frac{u(t)^2 + 2}{u(t)\sqrt{u(t)^2 + 4}} \quad ; \quad u(t)^2 = u_{min}^2 + \left(\frac{t - t_{max}}{t_0}\right)^2 , \quad (3)$$

where u_{min} is the impact parameter of the lensed star with respect to the lens in units of the Einstein radius, t_0 is the characteristic time of the event, and t_{max} is the time of maximum magnification. Woźniak & Paczyński (1997) show that the parameters $\{ f, u_{min}, t_0 \}$ form an approximately degenerate set, and since f is not known independently, the other parameters cannot be known either.

It has been suggested by one of us (Goldberg 1998) that in very crowded fields a large fraction of gravitational microlensing events will exhibit a characteristic astrometric shift. If an observed image is composed of two or more true stars, then the center of the PSF will be weighted toward the center of light of contributing stars. For an unblended or very weakly blended event ($f \simeq 1$), the center of light is essentially defined by the position of the lensed star. However, for a strongly blended event ($f \ll 1$) the lensed star may be almost anywhere within the PSF and not significantly affect the center of light.

As the magnification increases, the center of light will shift toward the lensed star. Thus, if we consider a blended image which is centered at the origin at baseline flux, and then lens a star within the image at $(\Delta x_0, \Delta y_0)$, simple geometrical arguments show that the center of light will shift toward the lensed star:

$$\Delta x = \Delta x_0 \frac{A_{obs}(t) - 1}{A_{obs}(t)} \quad ; \quad \Delta y = \Delta y_0 \frac{A_{obs}(t) - 1}{A_{obs}(t)} . \quad (4)$$

This effect has been observed; Alard (1996b) demonstrated a shift in DU0 # 2, a binary event which was known to be blended photometrically. However, astrometric shifts have not been more widely used, and indeed, there is a certain amount of skepticism that they may be significant (Han 1997).

Goldberg (1998) suggested that by looking at astrometric shift information from a microlensing event, we may approach the problem of blending in two ways. First, those events with larger shifts will tend to have a higher degree of blending than those with small shifts. Detailed models of a population can potentially yield a loose shift-blending relation. Second, by performing a best fit of equations (4) for Δx_0 and Δy_0 , we can find the position of the true lensed star with respect to the observed PSF and the local field. High resolution followup observations can then be used to determine the brightness of the lensed star, and give a direct measure of the degree of blending.

In this paper, we shall measure the astrometric shift for candidate microlensing events in the OGLE archive. Though we do not attempt to explicitly to calculate it here, any quantitative estimate of the optical depth of the galaxy to microlensing must include the effect of blending, and the presence or absence of a shift can provide a handle on this. Our outline is as follows. In § 2, we discuss our analysis methods, in particular, data reduction, photometry, and determination of the position shift. In § 3 we discuss the astrometric shifts found for the OGLE archive. Finally, in § 4, we discuss some interesting effects that we noted in this study as well as present some suggestions for future study.

2. Analysis

2.1. Data

Events analyzed in this paper are those reported by OGLE collaboration from the first stage of the experiment (Udalski et al. 1992) including objects caught on the spot by the “early warning system” (Udalski et al. 1994b). Woźniak and Szymański (1997; hereafter W& S) extracted from every frame in OGLE-1 archive a 100×100 pix subframe centered on objects which were formally variable only in one observing season and constant during remaining seasons. This dataset includes OGLE-1 microlensing candidates and is restricted to good quality frames (grades A-E, F frames rejected). Depending on the field it covers 3 or 4 seasons between 1992 and 1995, of approximately 4 months of observing each. The single Ford (Loral) 2048×2048 CCD with $15\mu m$ pixels used by OGLE team results in a scale of 0.44 arcsec/pix. A 44×44 arcsec subframe of a dense stellar field towards the Galactic center contains plenty of stars to allow difference photometry and good registering of the images. The images, as provided by W& S were de-biased and flat-fielded by an automated data pipe line based on IRAF “ccdred” routines. We refer to Udalski et al. (1992) and W&S for details of preliminary reductions, selection criteria and occasional exceptions.

2.2. Method

All of the remaining steps, that is profile photometry, cross identification of stars and registering of images were done independently. Previous data analysis of microlensing events has focused on identifying candidate events and using the best photometry possible to determine a light curve (and hence the microlensing parameters). The OGLE team used a fixed centroid template to “warm start” DoPHOT (Schechter et al. 1995) in order to maximize identification rate of the stars in dense fields (equivalent to the assumption that there is no shift !). To find the shift, however, we need to define an accurate “absolute” reference coordinate system and measure the position of the amplified star with respect to this system. Therefore we use DoPHOT in different mode and identify stars in each frame independently.

The outline of our method is as follows. For each of the 100×100 pix image, we create an observed catalog, that is the list of stars found by DoPHOT. The brightnesses and positions of stars we found in all subframes during unlensed period are used to generate a template catalog, a basis of the reference coordinate system. During the lensed period, the positions of the lensed star relative to the template are computed. Finally, errors in position and brightness were determined, and a best fit of equations (3) and (4) were computed.

2.3. Locating Stars and Photometry

We benefit from the analysis by the OGLE group in many ways, not in the least because we did not need to calculate a seeing and approximate sky level for each subframe, as this had already been done.

We divide the subframes into two categories: those during the event, and those preceding or following the event. Again, we have the benefit of the previously computed light curves. For those outside the event period (typically $|t - t_{max}| \gtrsim 2 t_0$), we select one of the “A” quality frames to serve as an initial template. Note that this frame is privileged primarily in the sense that all other frames will be rotated into the same coordinates.

The template catalog is adjusted iteratively. We begin with one frame, and add additional frames by determining a four parameter coordinate transform: $\{\theta_i, \delta x_i, \delta y_i, F_i/F_1\}$, that is rotation, parallel shift and flux ratio.

We determine the values of the transformation vectors by comparing the new stars to the template in order of decreasing brightness. As each star is added, it is rotated using the transformation matrix and compared to the previous template, and if the fit is acceptably

good (typically $\Delta r < 2$ pixels and differences in flux less than 20%), we iteratively adjust the transformation vector to minimize χ^2 over all the new stars. Otherwise, we throw out the star. This continues through the entire catalog. Typically, we were able to associate ~ 120 stars per subframe with the stars in the template. Once we have found the transformation matrix and assigned the new stars to the template stars, we recompute the position and brightness of each template star by taking the reference system resulting from an average of all the subframes observed thus far.

We perform this comparison for all the baseline subframes (typically ~ 100), and in the end we have well determined centroid positions and brightnesses for the template.

2.4. Finding the shift

For the subframes during the event, we want to be careful that we do not use the source star or any of its nearby neighbors to compute the transformation vector, since we *expect* a shift as a function of time. As such, we exclude the central 10×10 pixels around the lensed star for this calculation, but otherwise compute the transformation vector exactly as during the unlensed period. Once the transformation matrix is computed we transform the position and brightness of the source star to the template coordinate system.

An estimate of the errors in the shift for each subframe was determined by comparing stars similar (differing by less than 20%) to the source star in brightness *as measured in that frame* to their positions and brightnesses in the template catalog. We typically find 15 – 30 comparison stars per subframe, and their distribution is approximately Gaussian. As an estimate of the uncertainties in position, we take the dispersions around the known position of each comparison star.

In order to estimate the uncertainties in brightness, we used the magnitude uncertainty given by DoPHOT, multiplied by a correctional coefficient which takes the crowdedness into effect (Udalski et al. 1994a). Typically, these coefficients are ~ 1.2 .

Finally, we compute a best fit to equation (4) and, where applicable, equation (3). Note that we only use those data points which occur *during* the microlensing event. The unlensed frames are only used in computing the baseline positions and brightnesses. Uncertainties in Δx_0 and Δy_0 are estimated by:

$$\sigma_{\Delta x_0} \simeq \left(\frac{\partial \chi^2}{\partial \Delta x_0} \right)^{-1} \quad ; \quad \sigma_{\Delta y_0} \simeq \left(\frac{\partial \chi^2}{\partial \Delta y_0} \right)^{-1} \quad , \quad (5)$$

evaluated around the best fit values.

The uncertainties in the light curve parameters are computed by determining a covariance matrix for u_{min} , t_0 and t_{max} ; the associated errors are calculated in the standard way:

$$\sigma_i = [(\mathbf{C}^{-1})_{ii}]^{1/2}, \quad (6)$$

where,

$$C_{ij} = \frac{\partial^2 \chi^2}{\partial \alpha_i \partial \alpha_j}, \quad (7)$$

and α_i is the set of light curve parameters.

3. Results

Of the 19 candidate microlensing events reported by the OGLE collaboration, subframes were reduced for all but OGLE #13, which was not part of the normal search field, but rather was a followup of a MACHO event toward the galactic bulge (Szymański et al. 1994). OGLE #2 was on the boundary between the BWC and BW5 fields, and hence, we have two sets of subframes which are analyzed independently from one another.

Of the remaining events, OGLE #'s 4, 16, and 19 were not consistently detected using DoPHOT. This bears discussion. Since we did not use a template image to determine positions of stars, each frame was run independently, and thus dim source stars were not always detected. These stars had I magnitudes of $\simeq 19.3, 18.5, \& 19.6$, respectively. Likewise, the lack of a fixed template allowed the centroid to “move” due to local effects. One of the results of this is that, in general, we effectively had worse photometry than in the official OGLE catalog.

We summarize the results of the 15 observed events, including the double set of OGLE #2 in table 1. Throughout, all units of position are given in units of pixel lengths. Of the 15 events, 7 showed shifts of ≥ 0.5 pixels, not including OGLE #12, which will be discussed shortly. Some, such as OGLE #6 had such a large and well-defined shift, that is straightforward to pick out the slope even by eye. We also show the plots of the observed astrometric shift (in pixels) and the light curves for the events in Figures 1 and 2, respectively. It should further be noted that the microlensing light curves that we determined were generally quite similar to those computed by the OGLE collaboration. One primary reason for difference in our parameters may have been the use of a moving PSF. Since the integrated brightness is essentially a convolution of PSFs, it should be unsurprising that allowing a moving PSF will also allow for variation in brightness.

Many of the events have interesting, occasionally unexpected, behavior. First, there were 3 events which had obvious outliers: OGLE #'s 1, 3, and 14. In each case, there were points which were several σ from the best fit of equation (4). Moreover, photometrically, they clearly differed from the other points in the light curve. We removed the outliers only where there was a poor fit both astrometrically and photometrically. For the sake of completeness, we have plotted the outliers as open triangles in both Figures 1 and 2. An inspection of the frames containing the outliers reveal that they are primarily caused by a bad PSF, and CCD defects.

OGLE # 2 was measured twice, and since the shift was significant, (and indeed, consistent to within 1σ errorbars in both the x and y directions), this serves as an affirmation that we are, in fact, detecting a shift. Moreover, it suggests that our estimates on our uncertainties were not unreasonable.

OGLE #5 had a significant shift of ~ 0.7 pixels. This is quite encouraging as this event had been previously considered to be blended based on photometric information (Alard 1997).

OGLE #7 is a binary event, which the OGLE collaboration determined to be blended. They were able to perform a best fit to the binary lens microlensing parameters (Udalski et al. 1994c) using an observation of the event at the caustic crossing. We were unable to observe this point, and hence our photometry would be insufficient to uniquely determine the blending of the event. We did, however, detect a small astrometric shift of $\simeq 0.16$ pixels.

Near OGLE #12, we found a nearby (~ 3 pixels) dim star which was only occasionally observed. When it was not observed, the best fit of the source star was shifted toward the dim star. Thus, we find essentially two populations of images, one in which the companion is observed (12a), and one in which the companion is not observed (12b). Visual inspection of the frames reveals a CCD defect near the source image. Since the CCD is not aligned exactly the same with respect to the star field from night to night, some observations have this defect overlapping the source (in which case, the source is not observed), others have it nearby (in which case, the “companion” star is not observed), and others have it far away (in which case both are observed).

The surprising thing about these two populations is that when the companion is unobserved, and hence, when the event is *more* severely blended, we find that the baseline brightness of the source is $\sim 10\%$ dimmer than when the companion is observed. We believe that this is due to the fact that the centroid of the best fit PSF is shifted off the PSF of the source star, and hence, a non-negligible fraction of the light is being thrown out by DoPHOT.

The positions for both of the cases are given in coordinates with the weighted average center at the origin. Taking the two populations separately, we find that the center of 12a is (0.35 , 0.29), and the center of 12b is at (−0.37 , −0.29). Given that, the actual shifts for the two cases respectively are (−0.11 ± 0.09 , −0.15 ± 0.09) and (0.67 ± 0.09 , 0.82 ± 0.09). Thus, 12a has almost no shift. This, coupled with the fact that we have subtracted out a nearby star, suggests that the remaining measurement is essentially unblended.

Note that the values of Δx_0 and Δy_0 in table 1 are given in the same coordinate system, and hence we expect the 12a and 12b to have identical values of both, as Δx_0 and Δy_0 represent the physical position of the source star. Indeed, in the x coordinate, the two agree quite well. However, in the y coordinate, the two populations give inconsistent values to several σ . This is illustrated in Figure 1c, in which we would expect that the shift curves of the two observations will intersect at $(A_{obs} - 1)/A_{obs} = 1$ (infinite magnification), since observed position ought to be the same, whether or not the nearby companion is also observed.

This event is extremely interesting in that it points out the importance of accurate centroiding in photometric measurements. Since the PSF centers were fixed in previous studies, this has not been an issue. However, if this technique is to be more widely employed, the local environment, and the presence or absence of nearby stars must be carefully monitored.

Our light curves for OGLE #'s 14 & 18 are each extremely sparsely populated and of very poor quality. This is primarily due to the dimness (I=19, 18.7, respectively) of the stars. Though little confidence should be placed in our computed values for the microlensing parameters, we have included the curves for the sake of completeness.

4. Discussion and Conclusions

The primary result of this analysis seems to be a positive one. Astrometric shifts were found convincingly in over half the candidate microlensing events, some, such as OGLE #6, unambiguously detectable by eye. This confirms the belief that most events are significantly blended and that the majority of the events will show some measurable shift. Moreover, though we performed analysis on a particular dataset (OGLE-1), using an off the shelf image processing software package (DoPHOT), we suggest that the presence of an astrometric shift is a generic one, and that all projects toward the Galactic bulge, the LMC, or the SMC will show a significant fraction of events with large shifts. Further analysis could be used to provide an estimate of a statistical correction to the optical depth

of crowded fields to microlensing.

However, those events which show a shift may also be analyzed using followup analysis on a high resolution ground-based instrument. The detection of a shift gives the position of the source star in local coordinates with very high accuracy, and hence it becomes a straightforward matter to identify the correct source star in a high resolution image, and from that determine the value of f , and hence the other microlensing parameters, and the correction to the optical depth. Moreover, the very existence of a shift suggest which events are expected to be blended.

However, in doing this, we encountered several difficulties. First, we note that the local effects (eg nearby stars of comparable brightness) pose great difficulties in consistently measuring the position and brightness of the lensed star. Though this effect was pronounced in OGLE #12, it may have played a smaller role in other events and thus positional measurements are somewhat problematical.

Additionally, both local effects, and a dim source star can cause the star to be observed only intermittently. As a result, our uncertainties in Δx_0 and Δy_0 as well as the microlensing parameters are not measured with as high a precision as if the star had been detected on each subframe.

Moreover, photon statistics, crowding, and variable seeing, and so on, caused some difficulty in photometric measurements. Indeed, this is far from the ideal if one wishes to get optimum photometry. It should be noted, though, that the photometry does not artificially blend additional stars which were not blended in the initial OGLE measurements. If this were the case, we would measure a smaller amplification than in the OGLE catalog, which we do not.

One possible (and encouraging) way around these difficulties in measurement is frame subtraction (Alard & Lupton 1997). This method will ultimately provide a direct unshifted position of the source and unblended light in every frame.

In conclusion, we have shown that most events toward the galactic bulge do, in fact, have a significant astrometric shift. Moreover, we can conclude a high degree of blending. It is hoped that followup observations of this and similar analyses can help to provide greater accuracy in the measurement of microlensing optical depths.

The authors would like to gratefully acknowledge Bohdan Paczyński for invaluable discussions, and the OGLE team, in particular Andrzej Udalski and Michał Szymański for allowing us the use of their data. This research was supported by NSF grant AST-9530478, and DMG was supported by an NSF graduate research fellowship.

REFERENCES

- Alard, C. 1997, *A&A*, **326**, 1
- Alard, C. 1996a, *Astrophys. J. Letters*, **458**, L17
- Alard, C. 1996b, in Proc. IAU Symp. 173, *Astrophysical Applications of Gravitational Lensing*, (Eds: Kochanek, C. S. & Hewitt, J. N., Dordrecht: Kluwer), p. 215
- Alard, C. & Lupton, R. H. 1997, in preparation
- Alcock, C. et al. 1993, *Nature*, **365**, 621
- Alcock, C. et al. 1996, *Astrophys. J.*, **461**, 84
- Han, C. 1997, *Astrophys. J.*, astro-ph/9704212
- Di Stefano, R., & Esin, A. A. 1995, *Astrophys. J. Letters*, **448**, L1
- Goldberg, D. M. 1998, *Astrophys. J.*, in press, preprint astro-ph/9708172
- Paczyński, B. 1986, *Astrophys. J.*, **304**, 1
- Paczyński, B. 1996, *ARA&A*, **34**, 419
- Palanque-Delabrouille, N. et al. 1997, preprint astro-ph/9710194
- Schechter, P. L. Mateo, M. L., & Saha, A. 1995m *PASP*, **105**, 1342
- Szymański, M. et al. 1994, *Acta Astr.*, **44**, 387
- Udalski, A., Szymański, M., Kałużny, J., Kubiak, M., & Mateo, M. 1992, *Acta Astr.*, **42**, 253
- Udalski, A. Szymański, M., Stanek, K. Z., Kałużny, J., Kubiak, M., Mateo, M., Krzemiński, W., Paczyński, B., & Venkat, R. 1994a, *Acta Astr.*, **44**, 165
- Udalski, A., Szymański, M., Kałużny, J., Kubiak, M., Mateo, M., Krzemiński, W., & Paczyński, B. 1994b, *Acta Astr.*, **44**, 227
- Udalski, A., Szymański, M., Mao, S., Di Stefano, R., Kałużny, J., Kubiak, M., Mateo, M., & Krzemiński, W. 1994c, *Astrophys. J. Letters*, **436**, L103
- Woźniak, P. & Paczyński, B. 1997, *Astrophys. J.*, **487**, 55
- Woźniak & Szymański 1997, in preparation

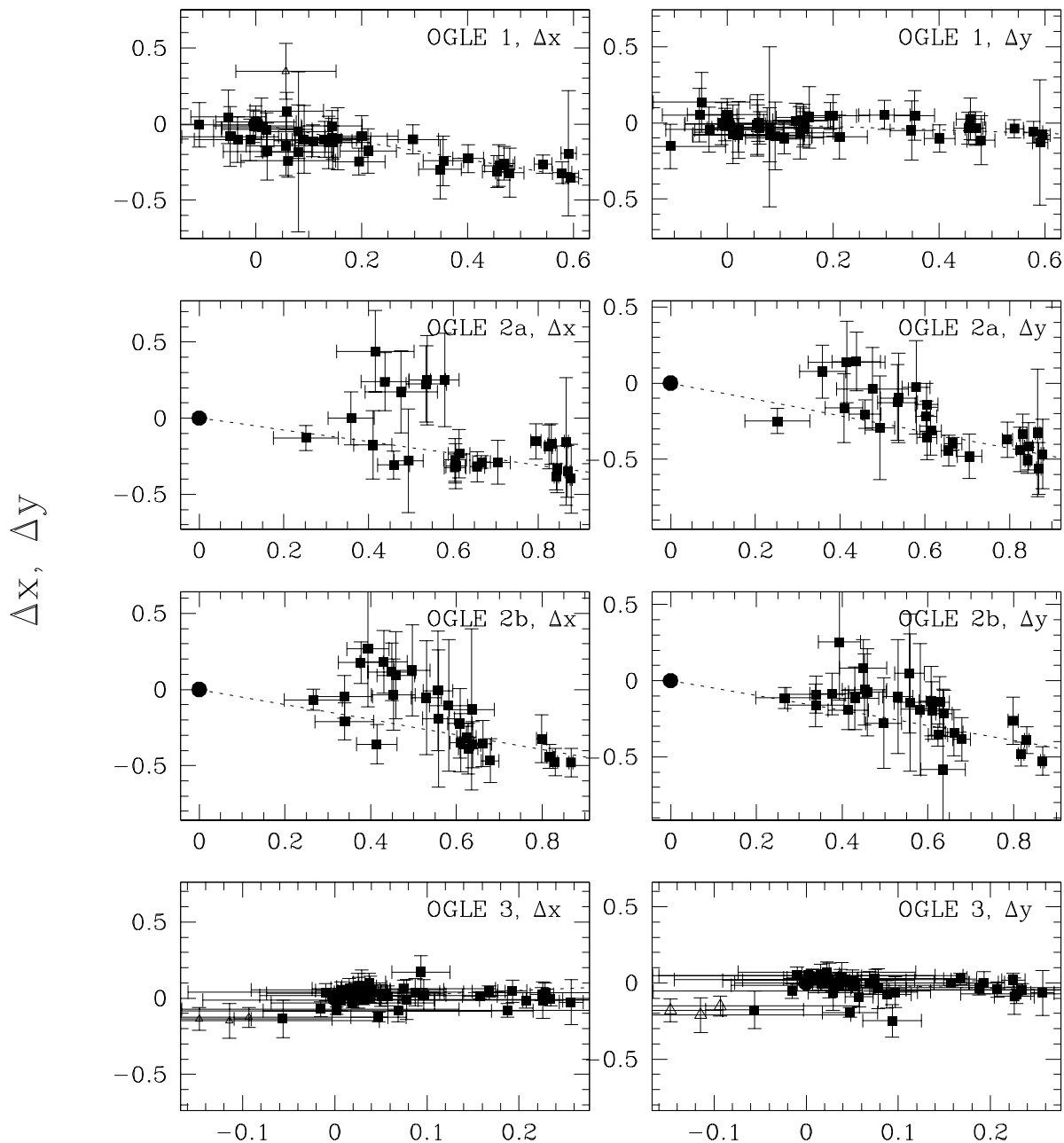
¹ OGLE #'s 1m 3 & 14 each have 1, 3, and 3 obvious outliers, respectively. In both cases, the outliers are both photometrically and astrometrically distinct from the rest of the population.

² OGLE #7 is a binary event.

³ Measurements of OGLE #12 are highly dependent upon detection of a nearby faint star. The interpretation of “events” 12*a* and 12*b* are discussed in the text

Table 1. A summary of the astrometric shifts and microlensing parameters of the observed OGLE events. Column 1 shows the event # used in the OGLE literature. Column 3 shows the number of frames in which the star is observed to be lensed. Columns 4 and 5 show the computed astrometric shift (equations [4]) in pixels, and the remaining columns give the computed microlensing parameters. Column 8 is the estimated date of maximum amplification in (J.D.-2448000).

#	Star #	obs.	Δx_0	Δy_0	A_{obs}^{max}	t_0 (days)	t_{max} (days)	χ_{min}^2
1 ¹	BW7 117281	38	-0.58 ± 0.04	-0.11 ± 0.04	2.60 ± 0.10	21.3 ± 1.2	1154.6 ± 0.8	17.6
2a	BW5 178651	26	-0.39 ± 0.04	-0.53 ± 0.04	8.51 ± 0.37	52.5 ± 1.8	803.3 ± 0.6	21.9
2b	BWC 10648	27	-0.49 ± 0.04	-0.49 ± 0.04	7.53 ± 0.35	48.2 ± 1.4	805.0 ± 0.5	34.7
3 ¹	BW3 161225	44	0.25 ± 0.07	-0.18 ± 0.07	1.30 ± 0.02	14.4 ± 1.5	833.7 ± 1.1	92.8
5	BWC 120698	20	0.64 ± 0.02	-0.34 ± 0.02	13.58 ± 0.16	12.7 ± 0.16	824.4 ± 0.2	85.1
6	MM5-B 128727	30	0.86 ± 0.06	0.09 ± 0.05	7.78 ± 0.3	9.3 ± 0.2	818.7 ± 0.1	53.6
7 ²	BW8 198503	29	-0.04 ± 0.01	0.16 ± 0.01				
8	BW9 138910	13	-0.83 ± 0.09	0.93 ± 0.12	1.56 ± 0.05	37.0 ± 5.9	1217.7 ± 5.1	2.4
9	MM7-A 86776	11	-0.30 ± 0.14	0.76 ± 0.15	1.75 ± 0.14	16.4 ± 4.9	815.0 ± 1.5	6.5
10	BW3 161220	44	-0.08 ± 0.08	-0.05 ± 0.09	1.11 ± 0.01	103.0 ± 21.4	840.1 ± 23.0	113.1
11	BW6 167045	33	-0.08 ± 0.10	-0.46 ± 0.15	1.28 ± 0.03	10.4 ± 2.0	1536.8 ± 1.9	16.4
12a ³	BW5 83758	27	0.23 ± 0.09	0.14 ± 0.09	1.94 ± 0.09	17.8 ± 1.4	1583.1 ± 1.0	30.9
12b ³	BW5 83758	34	0.30 ± 0.09	0.55 ± 0.09	2.13 ± 0.10	22.1 ± 1.4	1581.6 ± 0.9	74.0
14 ¹	MM1-A 123474	5	-0.5 ± 0.15	-0.43 ± 0.15	2.30 ± 0.36	25.0 ± 10.7	1815.9 ± 7.8	8.4
15	BW3 142477	19	0.46 ± 0.05	-0.64 ± 0.05	4.81 ± 1.68	16.9 ± 0.9	1854.2 ± 0.8	16.4
17	BW10 176006	30	0.00 ± 0.10	-0.05 ± 0.07	1.57 ± 0.15	139.9 ± 52.5	1975.7 ± 55.9	41.2
18	BW1 67895	6	-0.07 ± 0.25	3.35 ± 0.35	2.09 ± 6.6	21.2 ± 21.7	1914.5 ± 43.3	0.43



$$\frac{A-1}{A}$$

Fig. 1a.— The astrometric shifts in OGLE #'s 1 – 3. The dotted line shows the best fit to equations (4), yielding the values of Δx_0 and Δy_0 in Table 1. The solid circle shows the position and brightness of the source during the unlensed state.

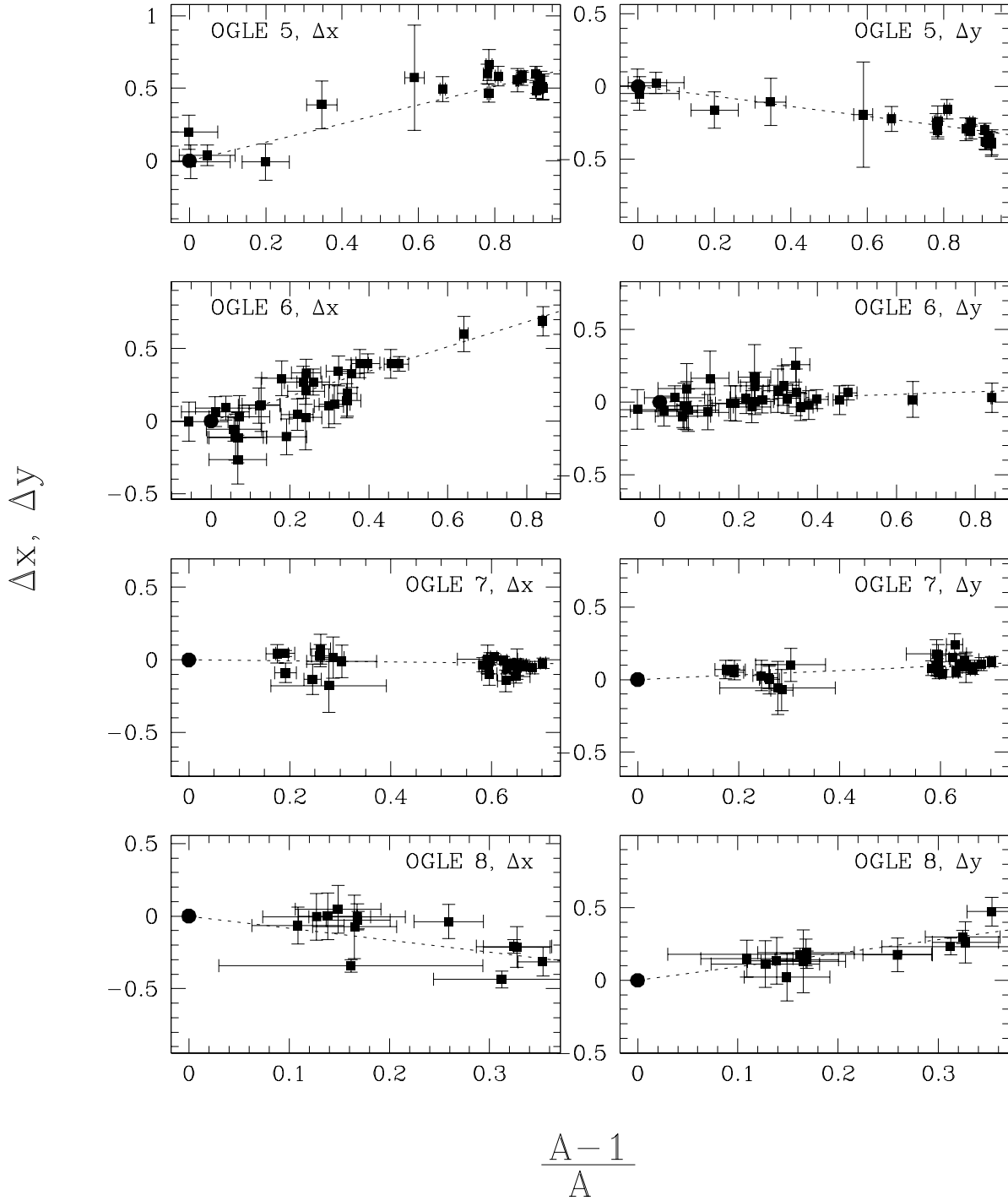


Fig. 1b.— As above, the astrometric shifts in OGLE #'s 5 – 8.

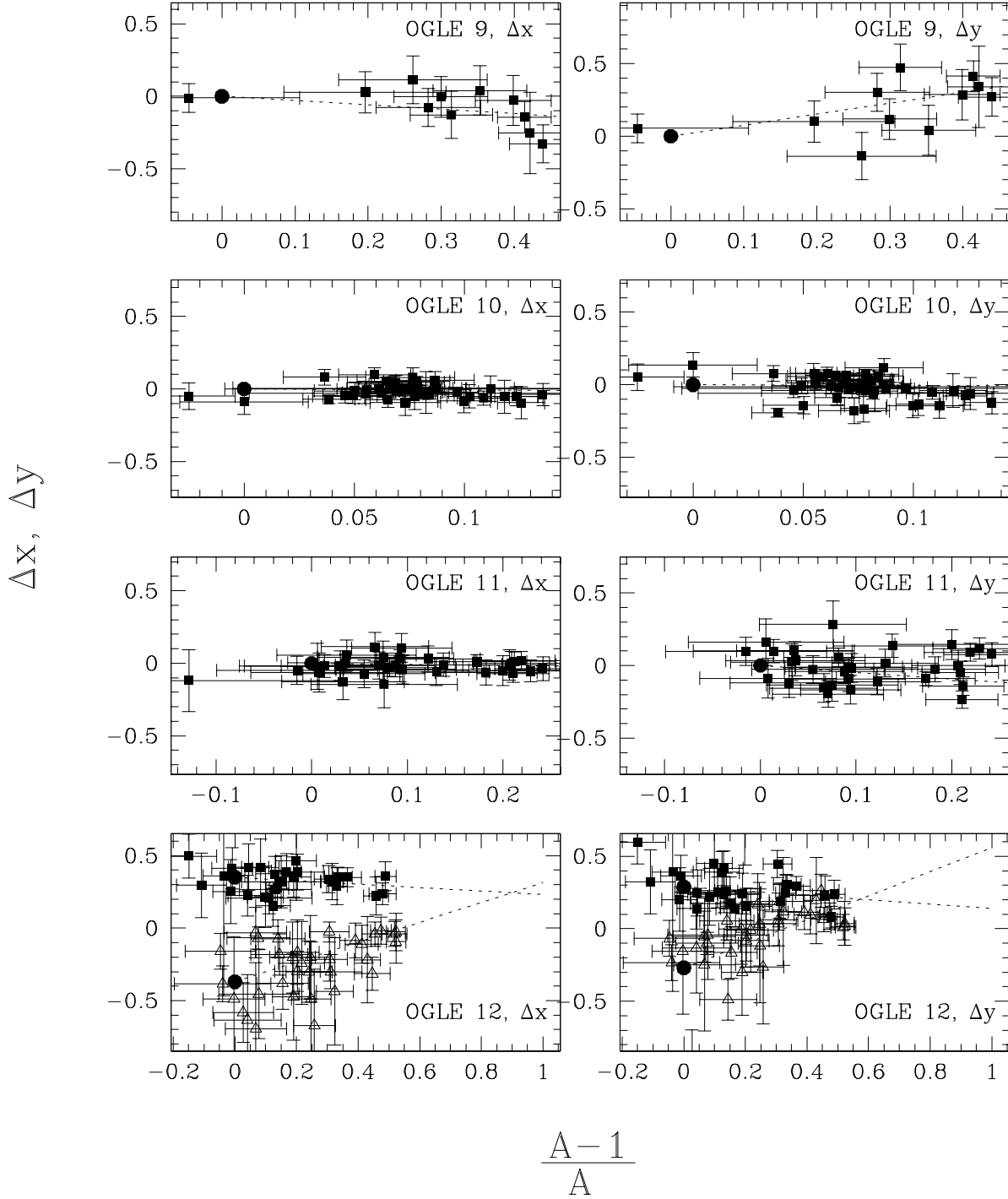
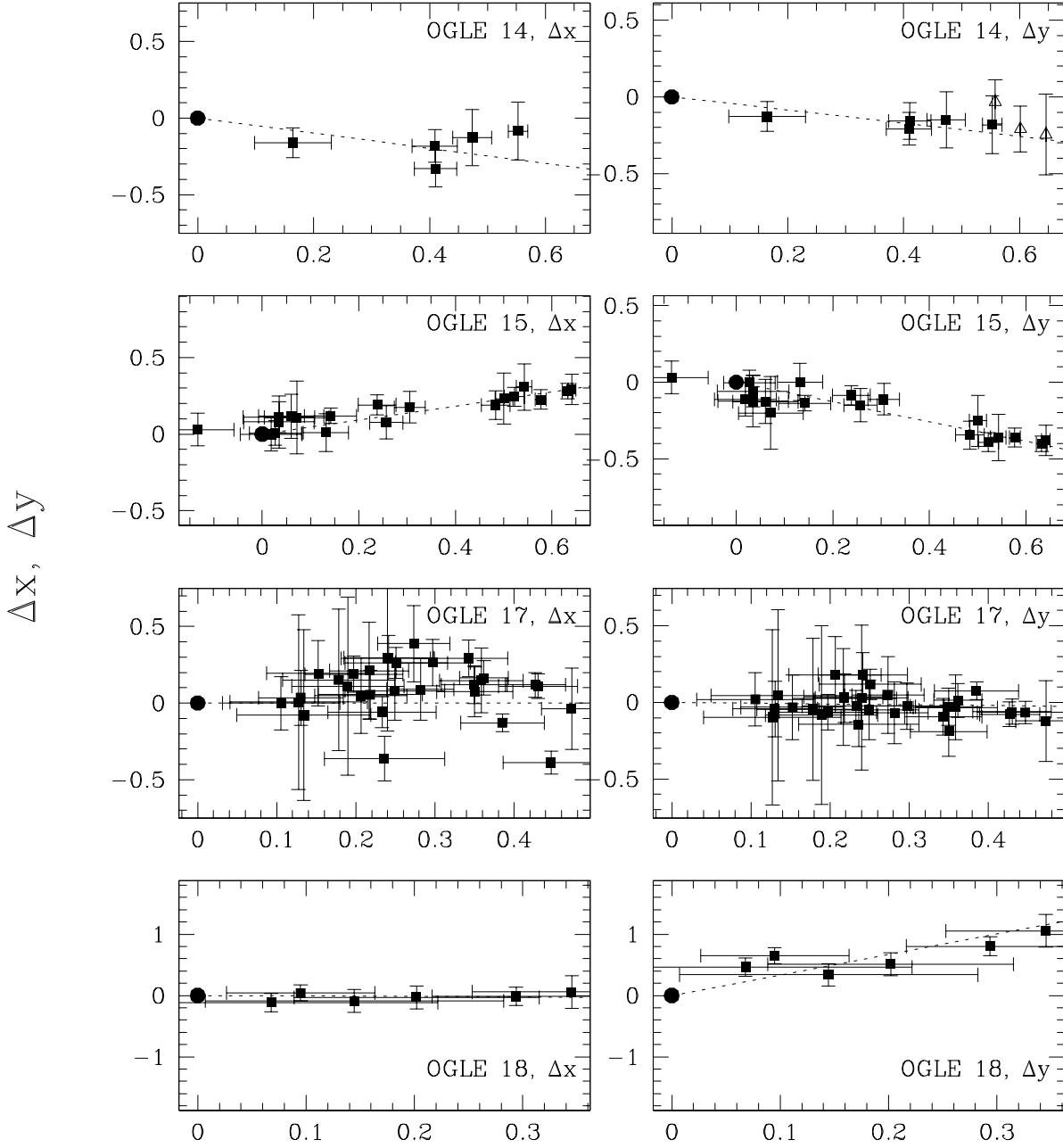


Fig. 1c.— As above, the astrometric shift in OGLE #'s 9 – 12.



$$\frac{A-1}{A}$$

Fig. 1d.— As above, the astrometric shift in OGLE #'s14 – 18.

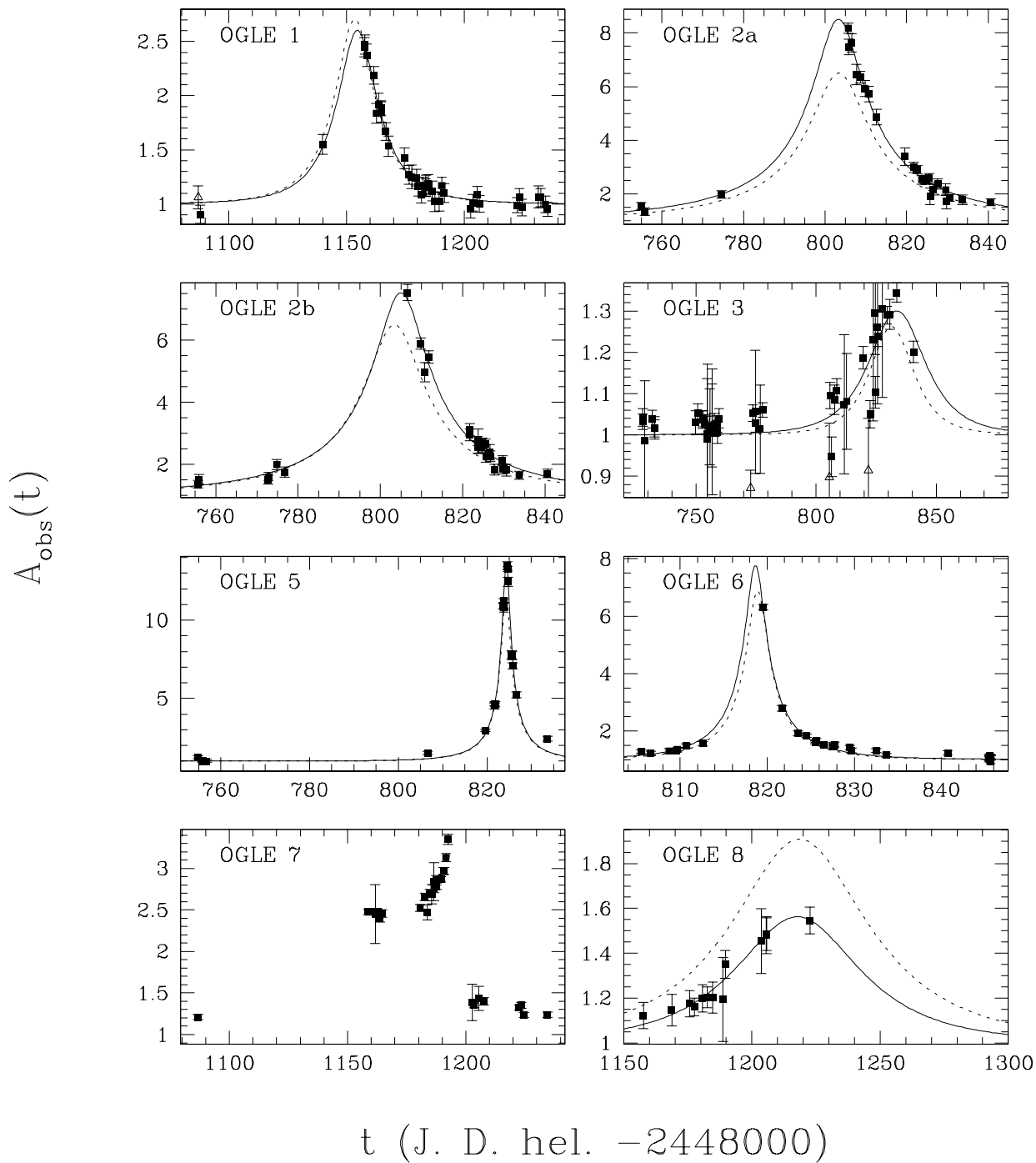


Fig. 2a.— The light curves for OGLE #'s 1 – 8. The solid line shows the newly calculated parameters, while the dotted line shows the OGLE parameters. The solid squares are our measurements of the magnification. OGLE 7 is a binary, for which we have not calculated microlensing parameters.

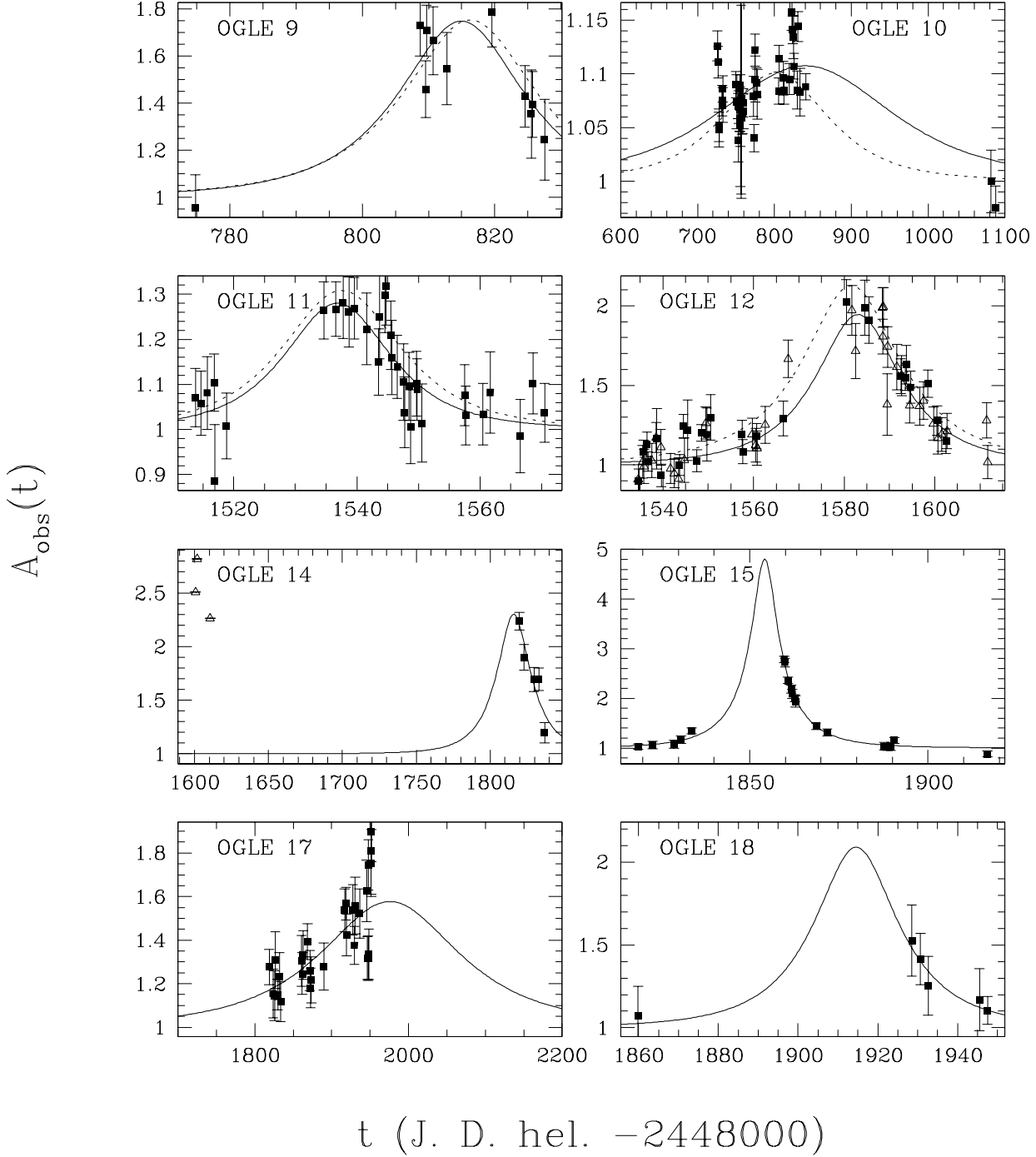


Fig. 2b.— As above, the light curve for OGLE #'s 9 – 18. Note, in OGLE 12, the solid squares and solid line correspond to OGLE 12a, the “unblended” realization discussed in the text. The dotted line and open triangles correspond to the case in which the nearby companion was not detected. For OGLE #'s 14 – 18, the OGLE group had not previously published a light curve.